



White Paper:

BIFACIAL VS SILICON MODULES ON GENIUS TRACKER™

The GameChange Solar Genius Tracker™ System was used for this study.
This work was supported by the U.S. Department of Energy under Contract
No. DE-AC36-08-GO28308 with the National Renewable Energy Laboratory (NREL).

Model and Validation of Single-Axis Tracking with Bifacial PV

Abstract

Single-axis tracking is a cost effective deployment strategy for large-scale ground-mount photovoltaic (PV) systems in regions with high direct-normal irradiance (DNI). The emergence of cost-competitive bifacial PV modules has raised the question of the additional value of bifacial modules in 1-axis tracking arrays. In this work it is shown that bifacial modules in 1-axis tracking systems boost energy yield by 7% - 15% depending on system configuration and ground albedo. This benefit is in addition to the 15%-25% energy gain already afforded by single-axis tracking relative to fixed-tilt deployments. Here we describe two models configured for bifacial (rear-side) irradiance estimation using one-axis tracking. We also compare model results against field performance data for two side-by-side bifacial and monofacial tracked systems – one in Albuquerque NM, and one in eastern Oregon. Albuquerque system shows monthly rear to front irradiance ratios between 10-14.9%. The results for Oregon indicate an average performance ratio 9.4% higher than a monofacial system. Results also show that smart tracking algorithms can offer more than 1% improvement on the yearly energy yield depending on location and albedo.

Index Terms — bifacial PV module, single-axis tracking, irradiance, configuration factor, ray tracing, model, performance.

I. Introduction

The solar market has seen a renewed interest in bifacial photovoltaic (PV) technology, which promises significant levelized cost of energy savings in comparison to conventional monofacial PV modules [1], [2]. Bifacial solar cells and modules can collect light from both sides including light reflected from the surrounding ground surface. This provides a degree of concentration and is beneficial for space constrained deployments. To some degree the increased output power off-sets the higher cost of manufacturing bifacial cells and modules compared to monofacial PV modules. Further cost reduction is expected through large scale manufacturing techniques. Glass-glass modules have also been predicted to have longer operational lifetimes due to better matching of the thermal properties of the package materials [3]. This may also reduce the levelized cost of energy from bifacial modules.

Bifacial modules can also be used in one-axis tracking systems to further increase energy yield and offset system cost. Bizarri [4] recently presented results from the La Silla PV plant in Chile, where a 550 kWp single-axis bifacial module array demonstrated a 12% increase in performance with respect to standard single-axis monofacial technology. Lindsay reports daily potential bifacial gains between 8%-14% for two single-axis trackers at Albuquerque, New Mexico [1]. This promising result suggests that further evaluation and optimization could lead to significant increases in energy yield for bifacial PV systems in one-axis tracking configurations.

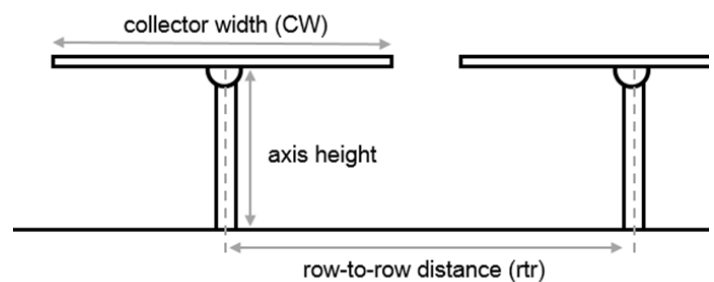


Fig. 1. On a tracking system, the fixed parameters are the distance between the centers of rotation, and the axis height. Module ground clearance, tilt, and separation between arrays varies with the solar position.

In this work, we compare measured field performance of several single-axis tracked bifacial systems with neighboring monofacial systems, and with modeled expectation based on two bifacial irradiance models. In prior work, we described a RADIANCE [5]-based ray trace model and configuration factor (CF) model [6] for rear-side irradiance. We also described a fixed-tilt systems, and verified them for fixed-tilt conditions with field data [6]-[8]. Here we extend these models for single-axis tracking applications.

The ray trace model offers the possibility of reproducing complex scenes, including tracker element shading. Run times of several seconds or minutes are possible with simple geometry and when using a cumulative-sky approach which calculates front-side and rear-side bifacial irradiance based on a single annual cumulative sky source for the year [9]. This composite source comprises all hourly Perez diffuse sky and direct solar contributions for the year. The CF model also incorporates the Perez tilted surface model [10], and assumes a 2D geometry to calculate the fractional irradiance entering and leaving the surfaces of an infinite-length PV array. This approach is also fast (~ seconds) but does not include complex shading or finite system edge effects.

Both models are freely downloadable [11], [12] and can be used to evaluate single-axis tracking scenarios. With single-axis tracking, the modules are no longer at a fixed tilt, and the clearances to the ground and with neighboring rows in the array are constantly changing. Tracking algorithms can be used to calculate these parameters, based on the ground coverage ratio (GCR):

$$GCR = \frac{CW}{rtr} \quad (1)$$

where CW is the PV collector width (overall width of the modules in a row), and rtr is the distance between the rotation axis of the panels as shown in Figure 1. GCR is used in tracking algorithms to implement backtracking corrections to the tilt of the trackers, based on minimizing shading from neighboring arrays. This correction becomes particularly important for arrays with higher GCRs. We can also define a normalized axis height H :

$$H = \frac{\text{axis height}}{CW} \quad (2)$$

These normalized parameters allow comparisons between tracker designs of different dimension (e.g. 2-up landscape vs 2-up portrait) since the self-shading geometry and bifacial rear irradiance is dependent on these normalized parameters, not on absolute dimensions.

Once the position of the tracker is known, the Perez tilted surface model can be recalculated for each configuration. For the raytrace model, a modified cumulative sky is used to determine the diffuse sky irradiance received by the array at different angles throughout the year.

II. Bifacial Models for 1-Axis Tracking

The tracking algorithm from PVLlib [13] is used to compute the array tilt for both the RADIANCE and CF models. Backtracking corrections have been employed to reduce self-shading of the panels throughout the day based on the ground coverage ratio (GCR) of the system.

A. Tracking CF Model

The CF model described in detail elsewhere [6] has been updated to allow for single-axis tracked bifacial systems. Given an array(s) with a specific axis height and orientation, the additional tracking-specific steps of the CF model are:

- Determining the array's tilt, ground clearance and row to row spacing with other arrays based on the specific time, location, and backtracking (optional).

- Identify the ground region that is shaded by the PV arrays under this configuration.
- Determine the irradiance received by the ground by accounting for shading and restricted view of the sky due to the tracker's position.
- Determine the irradiance for the backside of the PV module.

B. Tracking RADIANCE ray trace model

The Radiance bifacial PV model [11] has also been updated to allow for tracking systems. Additional steps include calculating the array tilt, ground clearance, and row-to-row spacing for each time step. The conventional fixed-tilt simulation workflow uses a single annual sky source to calculate annual average bifacial gain. For a tracked system, multiple scene geometries are required, along with the solar resource corresponding to each tracker tilt angle. Here we create separate simulation and scene geometry for each tracker tilt in 50 increments, along with the cumulative hourly solar resource corresponding to this solar zenith angle.



Fig. 2. Sandia bifacial tracking array with front and rear irradiance sensor shown (center). Two rows with GCR 0.28.

III. Field Comparison Systems & Method

Several bifacial tracking systems were investigated for this study. The first is a small-scale research array at Sandia National Laboratory, and the second is a set of 100kW commercial systems in eastern Oregon.

A. Sandia National Laboratory PV system

This deployment consists of two rows of 1-axis tracked bifacial modules. Reference cell detectors are mounted on the front and back of some of the modules to measure solar illumination. The tracker axis height is 0.5m, and the trackers are spaced from each other with GCR = 0.28. The ground albedo for the

site was unmeasured but assumed to be 0.25 for aged concrete. The field data are used to validate modeled G_{rear} / G_{front} using the CF model based on site-measured meteorological data.

B. Eastern Oregon Demo Site

Two commercial tracked systems east of Klamath Falls, OR are within 20 km of each other. One is composed of 100 kW of Silfab 285 bifacial modules in 2-up landscape, adjacent to 100 kW of Trina 300 W monofacial modules in 1-up portrait. The second system is composed of 200 kW of Silfab 285 bifacial modules, also in 2-up landscape orientation. Each system utilizes six Chint 36 kW inverters, with AC production monitoring. Hourly site irradiance satellite data is provided by The Weather Company's Cleaned Historical API for the purposes of performance ratio calculation.



Fig. 3. Oregon side-by-side bifacial site. $GCR = 0.35$, $H = 0.75$.

Inspection of the site geometry showed module collector width of 2 m and row spacing of 5.65 m, and a measured $GCR = 0.35$. Similarly, a 1.5 m tracker hub height measurement indicates a normalized axis height $H = 0.75$. Field IV curves were taken for one bifacial module in the center of a row under three different rear albedo conditions: rear irradiance completely blocked with black cloth; natural ground cover; and high reflectance (~80%) white ground cloth. Relative to the zero rear irradiance condition, natural ground cover increased module power by 10%, and reflective ground cover increased power by 20%, under mostly sunny conditions.

C. Field data comparison method

Bifacial system performance can be evaluated by comparing measured and modeled energy yield (Y_f) and performance ratio (PR) [14] for bifacial and reference monofacial systems. Measured AC electrical energy is aggregated for each site, excluding times when the site experienced inverter or tracker issues. Overall energy gain for a bifacial system is determined

by comparing energy yield Y_f [kWh/kW] for both monofacial and bifacial systems [15]:

$$BG_E = 100\% \times \left(\frac{Y_{f,bifi}}{Y_{f,mono}} - 1 \right) \quad (3)$$

Although BG_E gives a value of overall system performance advantage, not all of this gain is due to a system's bifaciality. Improved low-light efficiency and better temperature coefficient can improve performance as well and will be captured in the above equation. Therefore, isolating the bifacial response requires normalization of Y_f by modeled front-side performance for both module types. Here $Y_{f,model}$ is calculated with the PVLlib single-diode model [16], [17] using inputs of hourly site irradiance data, and STC (front-side only) module parameters. If proper model coefficients including temperature coefficient are included, $Y_{f,model}$ will reflect the non-bifacial aspects of performance that differ between two module types. Eq. (3) is re-written with a correction factor based on the front-only difference expected for the two module types, which will help isolate the energy gain due to bifaciality:

$$BG_{E,bifacial} = 100\% \times \left(\frac{Y_{f,bifi} Y_{f,mono,model}}{Y_{f,mono} Y_{f,bifi,model}} - 1 \right) \quad (4)$$

The $BG_{E,bifacial}$ field-measured energy yield value is used to validate the bifacial optical models described above which model G_{rear} . Here, measured $BG_{E,bifacial}$ is compared with $BG_{E,Model}$ where

$$BG_{E,Model} = \varphi_{Pmp} \times \frac{G_{rear} Y_{f,mono,model}}{G_{front} Y_{f,bifi,model}} (1 - \eta_{loss}) \quad (5)$$

For bifacial system performance modeling, G_{rear} and G_{front} are front and rear modeled irradiance, respectively, φ_{Pmp} is the PV module 1-sun bifaciality, (rear vs front power ratio) as defined in [18], and η_{loss} which accounts for additional bifacial loss terms such as shading loss and irradiance mismatch. Here η_{loss} is assumed to be zero, and G_{rear} is averaged across the back of the bifacial module.

IV. RESULTS

A. Model Comparison and System Optimization

The advantage of 1-axis tracking for high DNI climates is well established. Fig. 4 shows annual G_{rear}/G_{front} bifacial improvement for two modeled TMY3 climate conditions: Albuquerque, NM (high DNI), and Seattle, WA (low DNI). Both bifacial irradiance gain and front-side irradiance are reduced as tracker spacing is reduced, due to increased self-shading on the front, and

reduced ground reflected irradiance on the rear surface. For a modeled albedo = 0.25 and $H = 0.75$, in Albuquerque the rear irradiance ratio ranges from $G_{rear}/G_{front} = 8\% - 9\%$. In Seattle due to increased diffuse irradiance, $G_{rear}/G_{front} = 9.5\% - 11\%$.

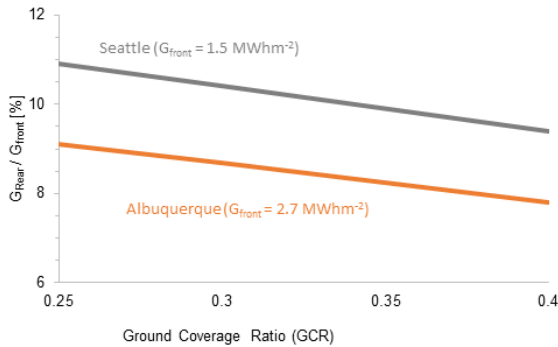


Fig. 4. G_{rear} / G_{front} irradiance modeled for two TMY3 locations. High GCR reduces rear bifacial gain (and front irradiance) due to self-shading. Assumed ground albedo: 0.25 (aged concrete).

The CF model was applied to evaluate tracker bifacial gain for many locations around the globe using satellite-based TMY irradiance data, and satellite-measured albedo values from NASA [19] (Fig. 5). The system configuration assumed was 0.35 GCR, $H = 0.75$. For some high-albedo equatorial locations, the gain from the 1-axis bifacial tracking was found to be as high as 20%, but a more typical global average value was 9%.

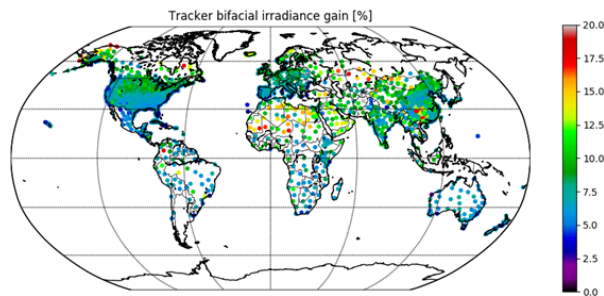


Fig. 5. Modeled G_{rear} / G_{front} [%] for 1-axis tracked systems over natural ground cover. Assumed geometry: $GCR = 0.35, H = 0.75$

B. Sandia National Laboratory Results

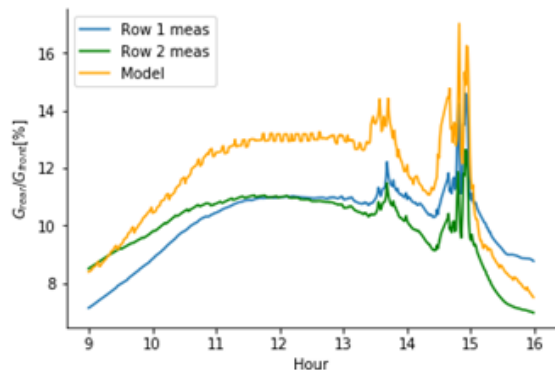


Fig. 6. Measured and modeled Bifacial Gain BGE% for March 30, 2017

Fig. 6 shows 5-minute measured and modeled G_{rear}/G_{front} for a single sunny day. It is clear that Row 1 is positioned to the east of Row 2 and therefore has a reduced G_{rear} in the morning when trackers are pointing east, and the backside has a view of the row behind. Likewise Row 2 has a reduced G_{rear} in the afternoon when trackers are pointing west and the back of the modules have an obstructed view due to the position of Row 1. Also visible is a large increase in measured BG_E for both rows during afternoon cloudy conditions. This further illustrates the increased bifacial gain that can be expected under cloudy conditions, or in climates with high diffuse irradiance fraction.

Cumulative rear vs front production is analyzed for seven months, and compared with $BG_{E, Modeled}$ using the CF model and on-site measure irradiance data. The cumulative measured BG_E shown in Fig. 7 is 11%, with monthly variation between 10-14.9%. The monthly $BG_{E, Modeled}$ varies little from month to month, with cumulative average = 12.3%. Measured values in May show anomalously large BG_E , potentially due to tracker misalignment reducing G_{front} during this month.

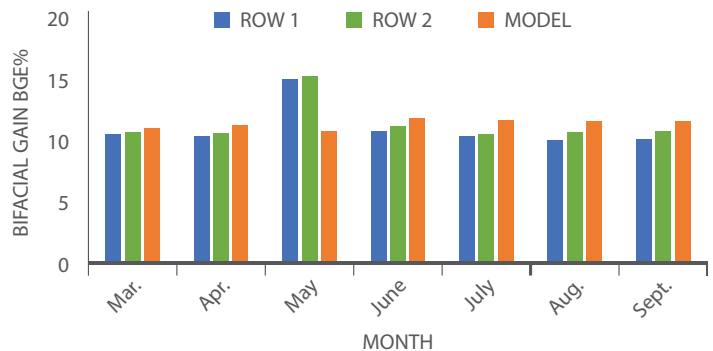


Fig. 7. CF model comparison vs SNL tracking systems from March to September. Anomalous large BGE in May could be due to tracker misalignment.

C. Eastern Oregon Data

AC energy yield data were collected for the side-by-side bifacial and monofacial installations. Performance Ratio (PR) values range from 0.63 to 0.90 for the two systems, with a cumulative average of 0.738 for the monofacial, and 0.807 for the bifacial systems. Although field IV curve measurements indicate comparable front-side capacity for the two systems, the measured PR was on average 9.4% higher for the bifacial system than for the monofacial system.

As mentioned above, system performance can be influenced by effects other than bifaciality, including temperature coefficient differences. To isolate bifacial gain, Eq. (4) is used, with expected system PR based on site temperature, irradiance, and module nameplate (front-side) parameters. These modeled PR

values are 0.777 for the monofacial, and 0.795 for the bifacial systems resulting in a corrected $BG_{E,bifacial} = 7.0\%$. This means that approximately 2.4% of the measured performance advantage of the Silfab HIT modules is due to improved front-side performance, rather than bifacial response.

Monthly $BG_{E,bifacial}$ values are shown in Fig. 8 based on measured AC energy production, as well as bifacial performance model results. Here, view-factor model hourly results are calculated based on site irradiance data and system geometry described in Section III. Site albedo is not known for certain, but based on tables of vegetation albedo [20], short grass typically has values of 0.15 – 0.25. Here a typical value of 0.2 is assumed. $\phi_{Pmp} = 0.95$ is also assumed, based on manufacturer datasheet estimates.

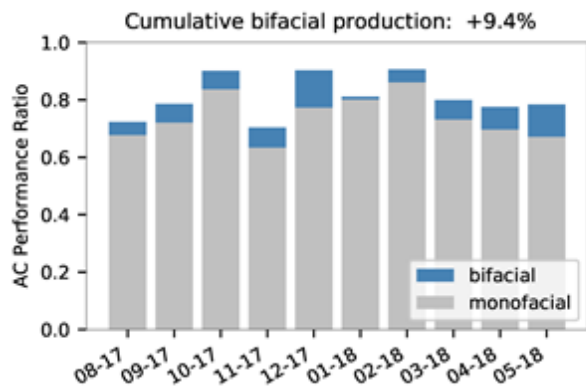


Fig. 8. Side-by-side production for two 100kW tracked systems. Bifacial PR ranged from 0.7 to 0.9 and averaged 9.4% higher than the monofacial system's PR.

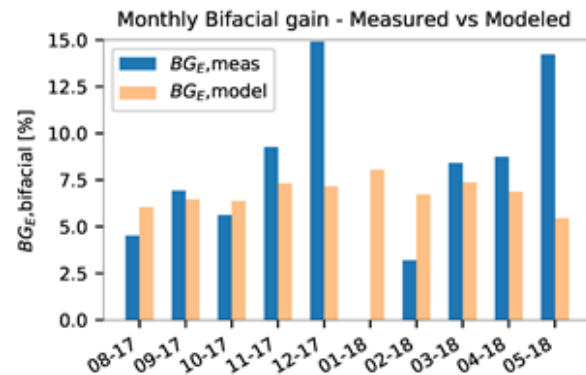


Fig. 9. Bifacial gain $BG_{E,bifacial}$ per Eq. (4) measured from AC production data, compared with CF bifacial energy gain estimates.

Figure 9 shows that on average, $BG_{E,Model}$ is 6.7%, which is close to the measured $BG_{E,bifacial}$ of 7%. However, monthly measured values had greater variability, particularly during the snowy winter months. In particular, December, January and May showed the greatest difference from the model. December likely showed greater than expected bifacial gain because of the high albedo ground cover that boosts rear-side reflected irradiance. However, January bifacial performance was particularly

bad. This underperformance was isolated to a 1-week period immediately following a heavy snow-storm where bifacial output was significantly below monofacial output. It is possible that snow was not shed from the landscape-oriented bifacial panels as quickly as from the portrait monofacial panels, which had a negative effect on the monthly comparison. The month of May is more difficult to explain, and may be related to other isolated performance issues with the monofacial reference system.

D. Bifacial-specific 1-axis tracker operation and gain

It has been previously shown for monofacial systems that optimized tracking algorithms can increase annual energy yield by up to 1% by moving the tracker off-sun closer to horizontal during cloudy conditions [21]. Gulin et al [22] showed that the optimal tilt angle can depend upon sky conditions and is not always horizontal. For bifacial tracking systems we investigate the possibility of similar optimized energy gain due to tracker alignment. For CF simulations in Klamath Falls (moderate irradiance), energy yield improvement is albedo dependent, varying from +0.6% at albedo 0.2, to +1.1% for albedo 0.8 (Fig. 10a). This improvement is location-dependant, and locations at higher latitudes and greater diffuse irradiance content (e.g. Seattle) can show more gain. Figure 10b shows how the instantaneous improvement in power occurs primarily on cloudy days.

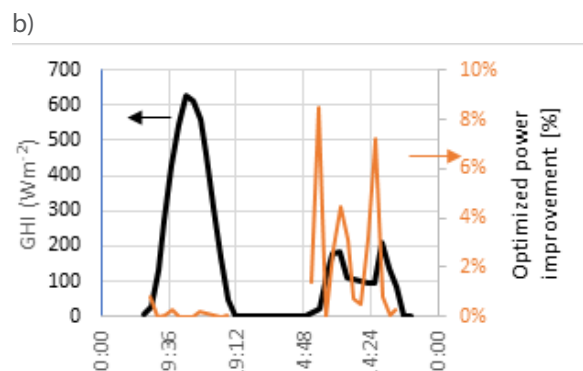
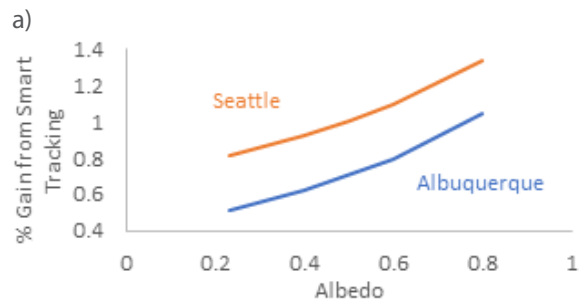


Fig. 10. a) Improvement in yearly energy capture from bifacial tracking systems for two locations, using optimized tracking. b) Power improvement for a sunny and cloudy day for Klamath Falls (May 5-6, 2017) by operating a tracker closer to 0 tilt under cloudy conditions.

E. 1-axis tracker irradiance nonuniformity

As described in [1], the rear irradiance for tracking systems can be significantly higher at the edges of the array. For small tracking systems like the Sandia array, the effect of the finite size of the array make significant differences with modeled results that assume infinite row extent and infinite number of rows like the CF model. Figure 11 investigates how many modules per row are required to meet the semi-infinite assumption at the center of the array for different clearances, finding that for any tracking height, 5 rows with 10 modules brings the G_{rear} within 5% of a semi-infinite assumption.

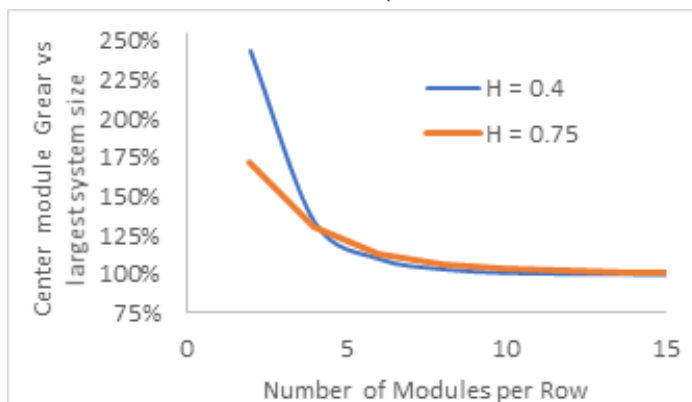


Fig. 11. BGE for small systems is compared with a semi-infinite (20 module, 7 rows) assumption. Edge effects for different normalized clearance height $h = H/CW$ and system sizes are evaluated through ray tracing. Seven rows assumed.

V. SUMMARY

A modification to the configuration factor and ray trace models was presented for estimating the total kWh/m² boost achieved in single-axis tracking systems when using bifacial modules. For model efficiency, the ray trace model generates multiple cumulative sky profiles that sum the hourly irradiance corresponding to different tracker tilts throughout the year. PVLib backtracking corrections to the tracking position for each time step was implemented to improve energy yield based on their ground coverage ratio. The models were described and benchmarked against measurements from two field deployments in New Mexico and Oregon. Both models agreed within 1%-2% for predicting the energy boost achieved. Modeling of the bifacial gains for different cities show a noticeable dependence on climate, and a reduction based on the ground coverage ratio.

ACKNOWLEDGEMENT

This work was supported by the U.S. Department of Energy under Contract No. DE-AC36-08-GO28308 with the National Renewable Energy Laboratory (NREL).

REFERENCES

- [1] A. Lindsay, "Modelling of Single-Axis Tracking Gain for Bifacial PV Systems," Eur. Photovolt. Sol. Energy Conf. (EU PVSEC), 2016.
- [2] M. Chiodetti, "Bifacial PV plants: performance model development and optimization of their configuration KTH," Thesis, pp. 1–77, 2015.
- [3] L. Yang, Q. H. Ye, A. Ebong, W. T. Song, G. J. Zhang, J. X. Wang, and Y. Ma, "High efficiency screen printed bifacial solar cells on monocrystalline CZ silicon," Prog. Photovoltaics Res. Appl., vol. 19, no. 3, pp. 275–279, 2011.
- [4] F. Bizarri, "Innovative bifacial pv plant at la Silla Observatory in Chile," 2017.
- [5] G. Ward, J., "The RADIANCE Lighting Simulation and Rendering System," 21st Annu. Conf. Comput. Graph. Interact. Tech., pp. 459–472, 1989.
- [6] B. Marion, S. Macalpine, and C. D. Nrel, "A Practical Irradiance Model for Bifacial PV Modules," 44th IEEE Photovolt. Spec. Conf., no. June, 2017.
- [7] C. Deline, S. MacAlpine, B. Marion, F. Toor, A. Asgharzadeh, and J. S. Stein, "Assessment of Bifacial Photovoltaic Module Power Rating Methodologies - Inside and Out," IEEE J. Photovoltaics, vol. 7, no. 2, pp. 575–580, 2017.
- [8] S. Ayala, C. Deline, S. Macalpine, B. Marion, J. S. Stein, and R. K. Kostuk, "Comparison of bifacial solar irradiance model predictions with field validation," Manuscr. Submitt. Publ., 2018.
- [9] D. Robinson and A. Stone, "Irradiation modelling made simple: the cumulative sky approach and its applications," PLEA - Passiv. Low Energy Archit. Eindhoven, Netherlands, no. September, pp. 19–22, 2004.
- [10] R. Perez, R. Seals, and J. Michalsky, "All-weather model for sky luminance distribution - preliminary configuration and validation," Sol. energy, vol. 50, no. 3, pp. 235–245, 1993.
- [11] NREL, "BifacialVF," GitHub, 2018.
- [12] NREL, "Bifacial_Radiance," GitHub, 2018.
- [13] W. F. Holmgren, R. W. Andrews, A. T. Lorenzo, and J. S. Stein, "PVLIB python 2015," in Photovoltaic Specialist Conference (PVSC), 2015 IEEE 42nd, 2015, pp. 1–5.
- [14] I. E. Commission and others, "Photovoltaic system performance monitoring-guidelines for measurement, data exchange and analysis," IEC 61724, 1998.
- [15] J. S. Stein, D. Riley, M. Lave, C. Hansen, C. Deline, and F. Toor, "Outdoor Field Performance from Bifacial Photovoltaic Modules and Systems."
- [16] W. De Soto, S. A. Klein, and W. A. Beckman, "Improvement and validation of a model for photovoltaic array performance," vol. 80, pp. 78–88, 2006.
- [17] R. W. Andrews, J. S. Stein, C. Hansen, D. Riley, C. Consulting, and S. N. Laboratories, "Introduction to the Open Source PV LIB for Python Photovoltaic System Modelling Package," pp. 170–174, 2014.
- [18] V. Fakhfour, "Photovoltaic Devices - Part 1-2: Measurement of Current-Voltage Characteristics of Bifacial Photovoltaic (PV) devices, IEC TS 60904-1-2 ED1, draft".
- [19] N. Aeronautics and S. A. (NASA), "Nasa Visible Earth catalog," EOS Project Science Office, 2018.
- [20] M. Iqbal, An introduction to solar radiation. Elsevier, 2012.
- [21] N. A. Kelly and T. L. Gibson, "Increasing the solar photovoltaic energy capture on sunny and cloudy days," Sol. Energy, vol. 85, no. 1, pp. 111–125, 2011.
- [22] M. Gulin, M. Vařak, and N. Perić, "Dynamical optimal positioning of a photovoltaic panel in all weather conditions," Appl. Energy, vol. 108, pp. 429–438, 2013.

Silvana Ayala Pelaez¹, Chris Deline², Peter Greenberg³, Josh Stein⁴, Raymond K. Kostuk¹

¹University of Arizona, Tucson, AZ, 85705; ²National Renewable Energy Laboratory, Golden, CO, 80401; ³NRGWise Lighting, Albany, OR 97321; ⁴Sandia National Laboratories, Albuquerque, NM, 87123;